

SUPPPORTING INFORMATION

LP/HT metamorphism as a temporal marker of change of deformation style within the Late Palaeozoic accretionary wedge of central Chile

T. HYPOLITO, C. JULIANI, A. GARCÍA-CASCO, V. MEIRA, A. BUSTAMANTE & C. HALL

Figure S1. (a) Zone of intense foliation transposition; note the intrafolial quartz veins marking previous foliation S_1 . (b) Andalusite porphyroblasts wrapped by S_2 foliation.

Figure S2. Bulk composition of metasedimentary rocks from the Chorrillos and Tanumé areas plotted on AFM (left) and AKF (right, larger symbols) diagrams (projected from coexisting phases and appropriate compositional vectors, see text for explanation). The plotted end members of phases of interest include those relevant for the lower-grade zones of the thermal overprint in the study area (Aguirre *et al.*, 1972; Willner, 2005; this work). The dashed circle in the biotite solid solution phase field shows the measured biotite composition (Table S1b). In the AKF diagram, muscovite compositions, which are represented by smaller symbols than whole rock compositions, are displaced towards A apex showing the influence of pyrophyllitic ($K^{XII} + Al^{IV} = \square^{XII} + Si^{IV}$) substitution and/or a paragonite component.

Figure S3. Bivariant diagram showing chemical variation in white mica from the Chorrillos and Tanumé areas. There is a tendency for the Na content to increase as Si decreases from the low-Al pelites (biotite zone) to Al-richer pelites (staurolite-andalusite zone). See text for clarification.

Figure S4. AFM diagrams for selected samples from the biotite, garnet–oligoclase and staurolite–andalusite zones. The equilibrium mineral assemblages are indicated by the tie lines connecting mineral compositions. Bulk-rock compositions are also plotted. Olig.=oligoclase.

Figure S5. Incremental step heating analysis of phengite of blueschist sample DTH-86G. See text for details.

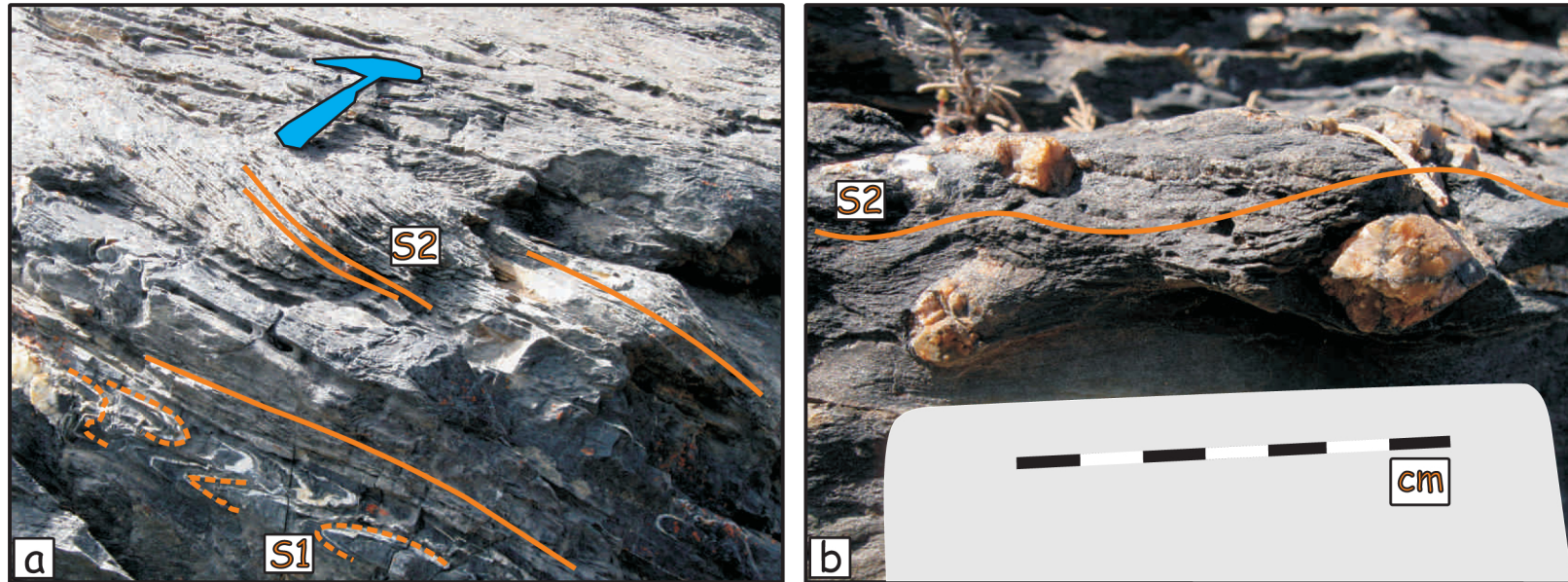


Figure S1. (a) Zone of intense foliation transposition; note the intrafolial quartz veins marking previous foliation S1. (b) Andalusite porphyroblasts wrapped by S2 foliation.

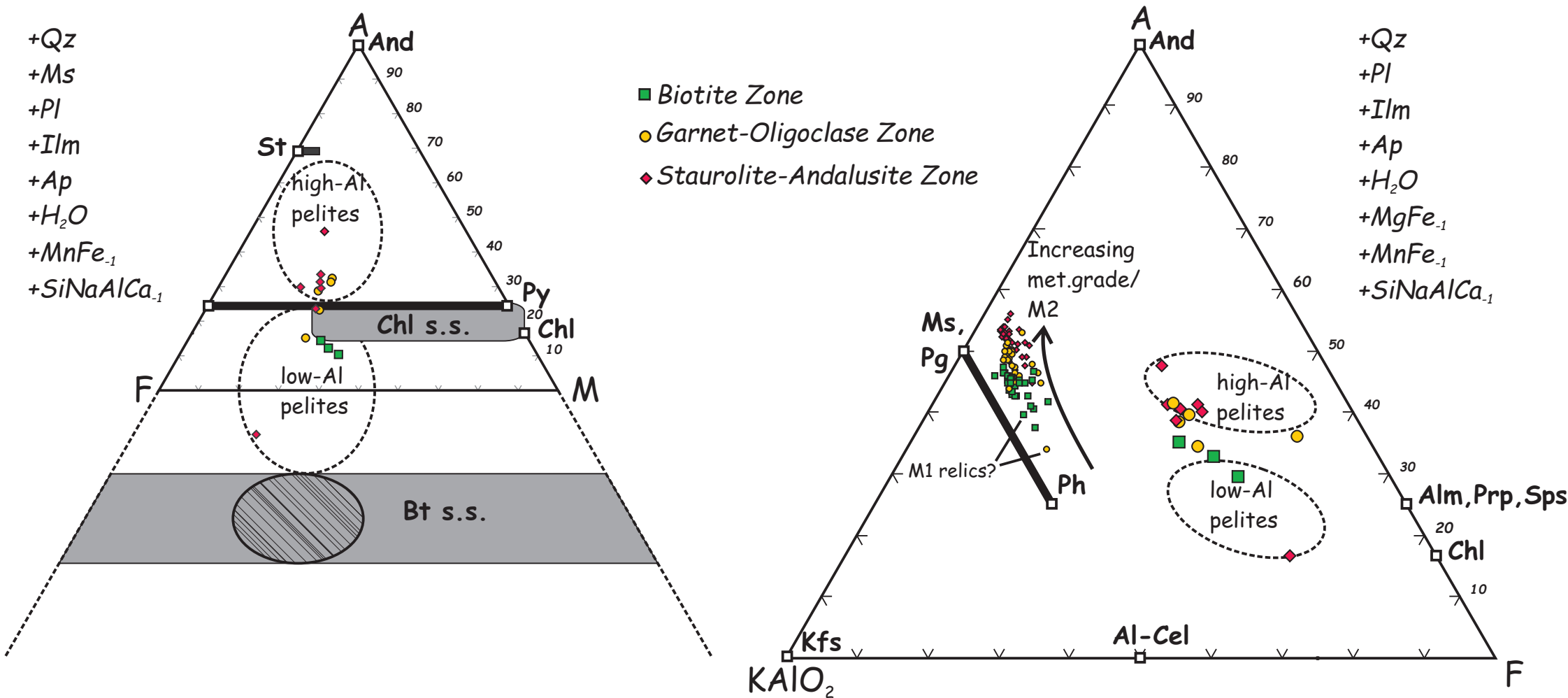


Figure S2. Bulk composition of metasedimentary rocks from the Chorrillos and Tanumé areas plotted on AFM (left) and AKF (right, larger symbols) diagrams (projected from coexisting phases and appropriate compositional vectors, see text for explanation). The plotted end members of phases of interest include those relevant for the lower-grade zones of the thermal overprint in the study area (Aguirre et al., 1972; Willner, 2005; this work). The dashed circle in the biotite solid solution phase field shows the measured biotite composition (Table S1b). In the AKF diagram, muscovite compositions, which are represented by smaller symbols than whole rock compositions, are displaced towards A apex showing the influence of pyrophyllitic ($K^{XII} + Al^{IV} = \square^{XII} + Si^{IV}$) substitution and/or a paragonite component.

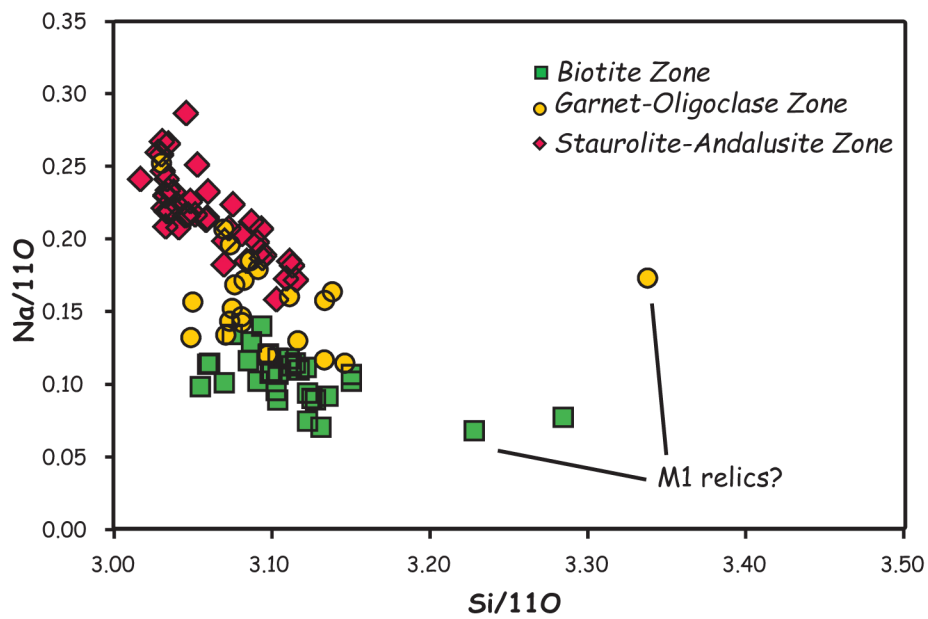


Figure S3. Bivariate diagram showing chemical variation in white micas from the Chorrillos and Tanumé areas. There is a tendency for the Na content to increase as Si decreases from the low-Al pelites (biotite zone) to Al-richer pelites (staurolite-andalusite zone). See text for clarification.

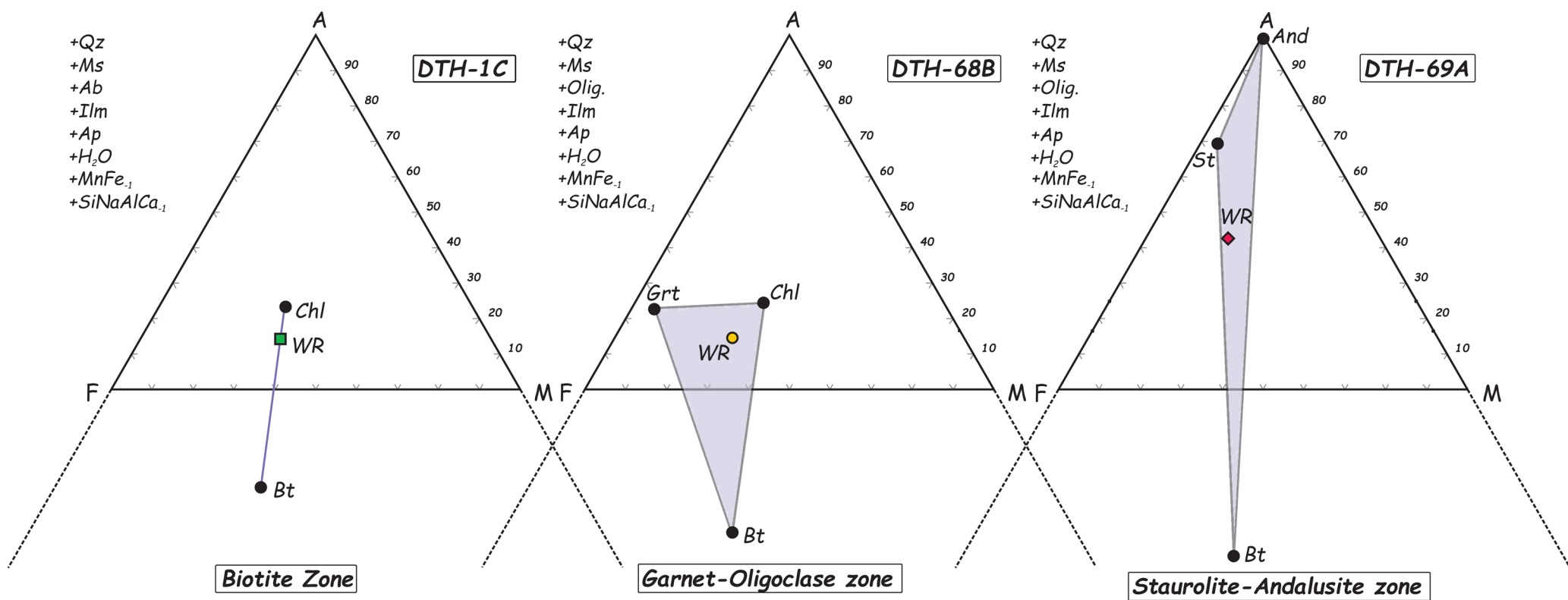


Figure S4. AFM diagrams for selected samples from the biotite, garnet-oligoclase and staurolite-andalusite zones. The equilibrium mineral assemblages are indicated by the tie lines connecting mineral compositions. Bulk-rock compositions are also plotted. Olig.=oligoclase.

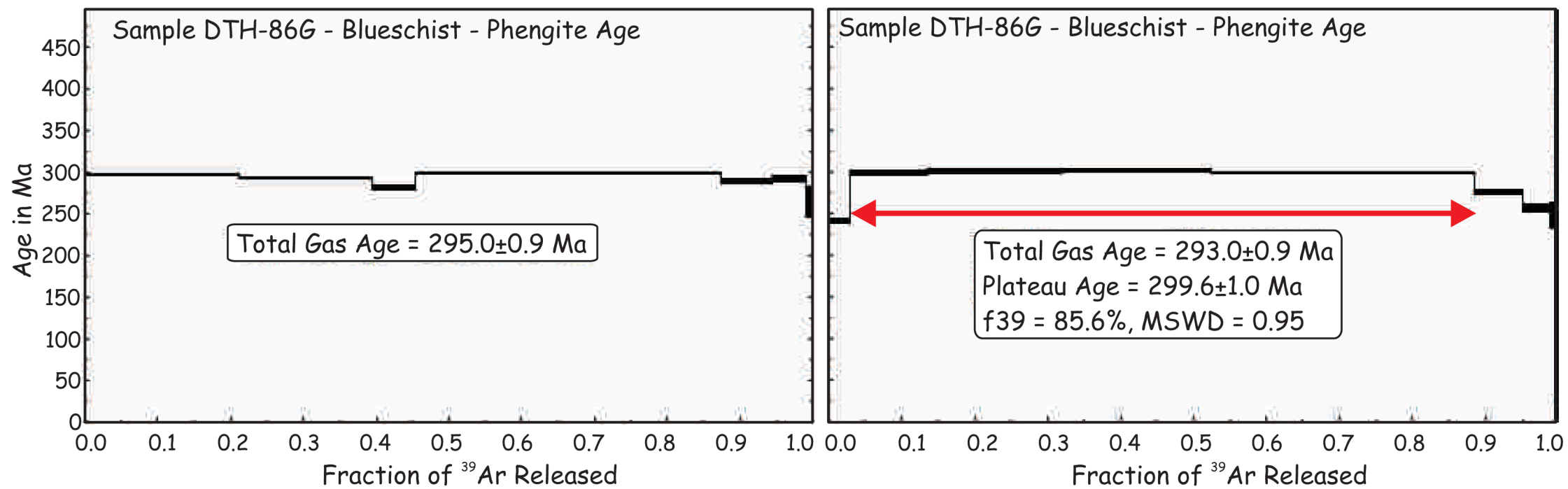


Figure S5. Incremental step heating analysis of phengite of blueschist sample DTH-86G. See text for details.